

## An Embroidered Passive Textile RFID Tag Based on a T-Matched Antenna

Mohamed El Bakkali<sup>1, \*</sup>, Otman El Mrabet<sup>1</sup>, Mohammed Kanjaa<sup>1</sup>,  
Ignacio Gil<sup>2</sup>, and Raúl Fernandez-Garcia<sup>2</sup>

**Abstract**—This paper addresses the design and fabrication of an embroidered textile RFID tag antenna. The main feature of this design is that we have embroidered an RFID chip on the textile support which avoids the use of metallic wires or soldering. The modeled equivalent circuit of the tag is presented to get physical insight into RFID tag antenna design. The detailed results given in this paper include the effect of the bending and the human body proximity on the antenna performance. It is shown that the bending does not introduce a conspicuous effect on the tags read range while the dissipative characteristics of the human body cause a gain and read range reduction. The proposed design may find applications in wearable devices dedicated to health monitoring applications.

### 1. INTRODUCTION

Radio frequency identification (RFID) is nowadays a widely deployed technology, used not only for tracking items on supply chains [1] but also as a background for more elaborate sensing technologies as WSN and more complex structures as IOT devices [2]. An emerging field of application of this technology resulted from the need of wearable health care systems. In this scenario, RFID tags would enable real time bio-monitoring of physiological parameters of medical patients in a non-invasive manner. The passive RFID tags used in such UHF-RFID systems are combined to a variety of integrated sensors. The physiological data are retrieved by the sensors and then conveyed by the tag wirelessly to the reader [3].

In order to be efficient in real body worn systems, RFID tags must satisfy at least three basic criteria: The body worn part of the system must be comfortable to wear, light weight, low profile, and inexpensive in order to be largely deployed. An efficient response to the latter requirements is given by electro-textiles or more precisely by RFID tags consisting of embroidered structures based on conductive threads [4]. Embroidered RFID tags can be seamlessly integrated to garments enduring any abnormal crumpling without affecting the tag structure when it recovers its original shape. A major issue that could reduce the efficiency of the embroidered antennas including the tags is that it is conceived to operate at close distance from the dissipative human body, resulting in an impaired radiation pattern [5]. Another issue results from the flexibility of the embroidered tag causing a variation of the geometrical properties of the tag. Both problems could highly affect the read range of the UHF-RFID tag antenna, yet the read range of the wearable UHF RFID tags is paramount in health body worn applications. In [6], authors evaluated the variation of the read range from 4 meters in free space to an average of 1.4 meters on human body. In [5], an analysis of the wearable tag performance at close vicinity human body was carried out. It was shown that the human body strongly affected the read range of the tag and considerably reduced the gain. In [7], both the permittivity and conductivity of

---

*Received 14 September 2021, Accepted 7 December 2021, Scheduled 21 December 2021*

\* Corresponding author: Mohamed El Bakkali (elbakkali.mohamed-etu@uae.ac.ma).

<sup>1</sup> Information and Telecommunication Systems Laboratory (LaSiT), Faculty of Sciences, Abdelmalek Essaadi University, Tetuan, Morocco. <sup>2</sup> Department of Electronic Engineering, Universitat Politècnica de Catalunya, Terrassa, Barcelona, Spain.

the human body were proven to directly affect the RFID tag read range, and a reference copper tag was used as a standard to gauge the response of an embroidery RFID tag on different human body locations. The results gave a measured read range of 1.5 meters with a negative gain. The studies in [8–10] show that human body absorbs an important amount of the forwarded energy from the power source which consequently causes a noticeable decrease in the antenna gain and efficiency. All the previous works concluded that the vicinity of the human body is the cause of a strong absorption of energy and causes gain and efficiency reduction to a value more than 50% of the results measured in free space.

The work presented in this paper is twofold. First, we studied the effect of bending on textile UHF-RFID Tag Antenna, since the spatial configuration of the antenna is capital in shaping its radiation pattern. Then, we proceeded to study the effect of the dissipative properties of the human body on the tag efficiency. First, a simulation of the bending effect is carried out using commercial software CST before proceeding to the final fabrication. The read range and gain of the RFID tag are simulated on different locations of the human body. The simulated results depict that the gain of the tag has decreased from 2.196 dBi to an average of  $-5.7$  dBi, and consequently, the simulated read range is reduced from 6.2 meters to about 1.7 meters. To confirm the obtained results, the read range measurement on human body is carried out in an office environment to match the real-life application scenario. The antenna is modeled with lumped element circuit to evaluate the effect introduced by the matching element.

## 2. ANTENNA DESIGN

The studied antenna is based on a conductive yarn embroidered as a weave fill stitch type (stitch spacing 0.5 mm, stitch length 4.35 mm) on a textile felt fabric used as a substrate material with a dielectric constant  $\epsilon_r = 1.2$ , loss tangent  $\tan \delta = 0.0013$ , and thickness  $h = 0.7$  mm, and the yarn corresponds to a commercial Shieldex 117/17 dtex 2-ply, which is composed by 99% pure silver-plated nylon yarn 140/17 dtex with a linear resistance  $< 30 \Omega/\text{cm}$ . The fabrication is carried out using an embroidery machine named Singer Futura XL550 as shown in Figure 1(a), and the prototype fabricated is shown in Figure 1(b). The light weight of this tag (Figure 1(c)) makes it suitable for wearable applications.

The main feature of this design is that we have embroidered the RFID chip on the textile support

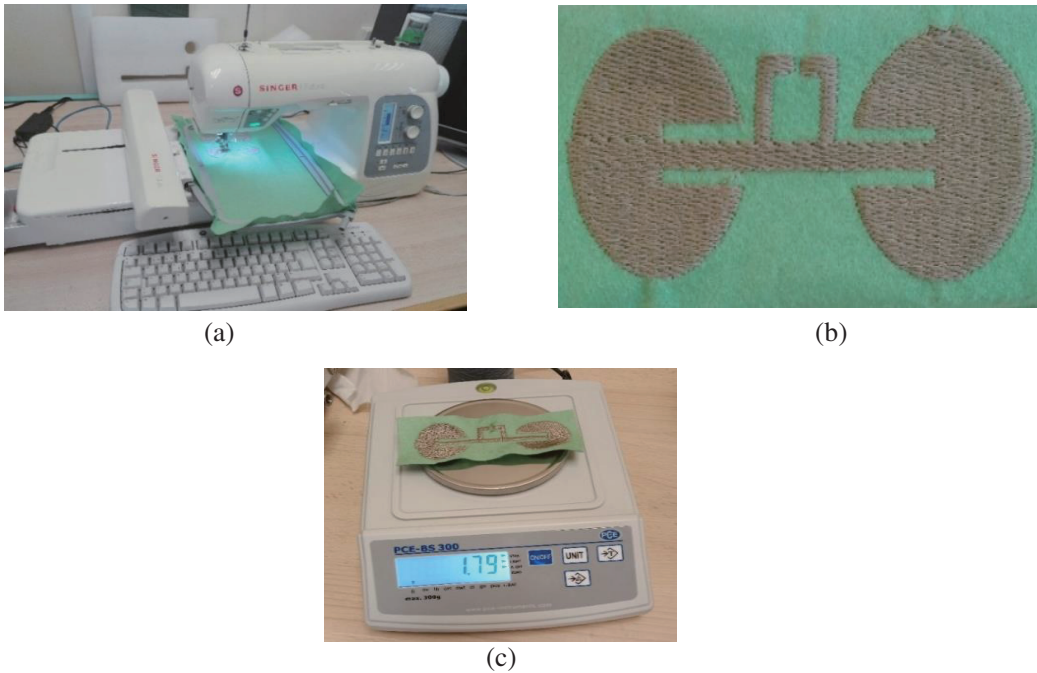


**Figure 1.** The fabrication process and resulting antenna. (a) Fabrication process. (b) Fabricated prototype. (c) Weight measurement in gram (g).

which avoids the use of metallic wires or soldering between the antenna and RFID chip. This technique leads to a quick, easy, and low-cost fabrication. Another feature of this technique is that it increases the durability of the proposed design in real life applications and enables it to endure harsh environments like washing machines. The proposed design has been optimized using a commercial software CST Microwave studio based on Finite Integration Method (FiT). The final optimized values are summarized in Table 1.

**Table 1.** Antenna parameters in millimeter.

| Parameter   | Size (Millimeter) |
|-------------|-------------------|
| $L_d$       | 64                |
| $D$         | 12                |
| $L_t$       | 9                 |
| $W_t$       | 18                |
| $W_d$       | 4                 |
| Slot        | 20                |
| $W_s$       | 3                 |
| Disk radius | 18                |

### 2.1. Slot Dimension's Effect on the Antenna Impedance

The antenna prototype is fabricated after studying all the matching parameters introduced (slots and T-matching element). The designed antenna consists of a dipole and two circular patches connected at each terminal of the dipole as shown in (Figure 2). Since the RFID chip reactance is roughly capacitive, an inductive reactance must be introduced by the antenna to ensure a maximum energy transfer to the RFID IC [10]. For this reason, two symmetrical slots are added to each circular patch in order to provide the required inductive effect. The optimal value of the slots is obtained by performing a parameter sweep simulation of the slots length from 5 mm to 20 mm. The obtained results presented in Figure 3 show that with a slot with a length of 20 mm the antenna input impedance achieves  $(18.9+j109.2) \Omega$  which is the closest value to the RFID chip MURATA (LXMS31ACNA-010) with an input impedance of  $(17.6-j105) \Omega$  at 915 MHz.

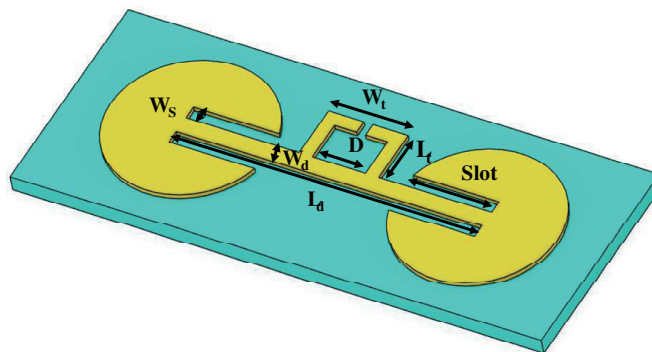


**Figure 2.** Design of the proposed antenna.

### 2.2. Tag Modeled Circuit

The T-matching element (See Figure 2) is based on the well-established technique that guaranties an easy control of resonance frequency. In other words, it facilitates a good conjugate matching between the RFID chip and the antenna, while reducing the dimensions of the antenna and getting a wider

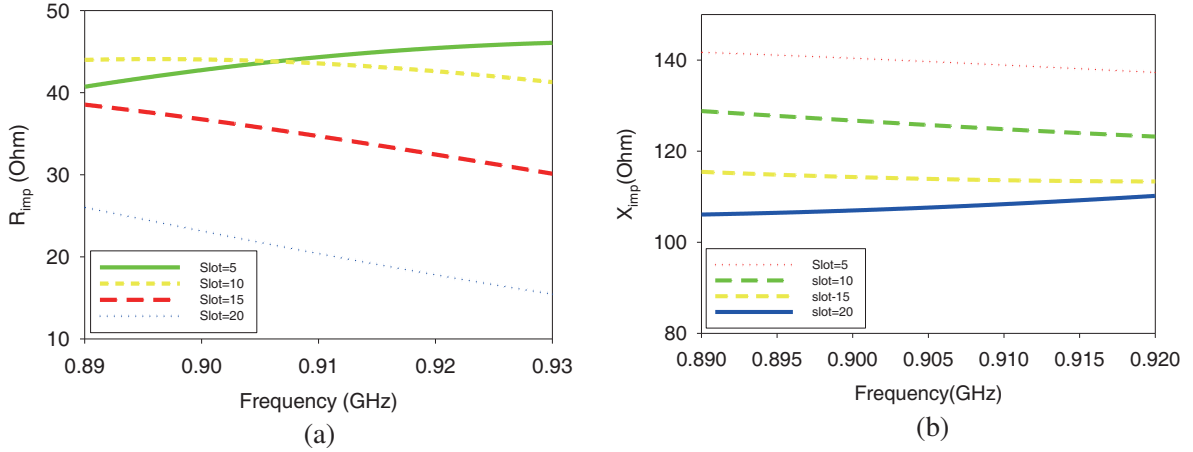


**Figure 3.** Effect of the parameter Slot on the input impedance of the textile RFID tag antenna: (a) real part, (b) imaginary part.

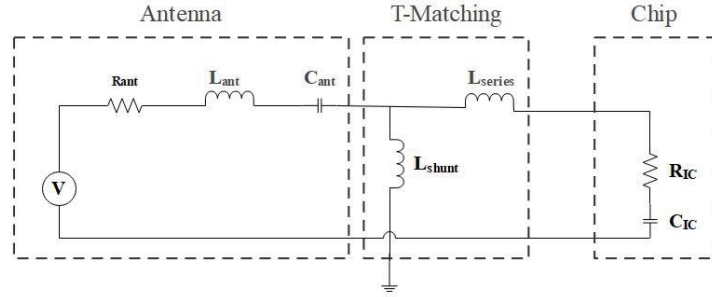


**Figure 4.** Modeled equivalent circuit of the textile RFID tag antenna. The values of lumped elements are:  $R_{ant} = 30.73 \Omega$ ,  $L_{ant} = 43.21 \text{ nH}$ ,  $C_{ant} = 0.67 \text{ pF}$ ,  $L_{series} = 16 \text{ nH}$ ,  $L_{shunt} = 6.98 \text{ nH}$ ,  $R_{ic} = 17.6 \Omega$ ,  $C_{ic} = 1.64 \text{ pF}$ .

bandwidth. In order to get physical insight into this RFID tag antenna design, an equivalent circuit is developed as shown in Figure 4. The T-matching element is modeled by two inductors ( $L_{shunt}$  and  $L_{series}$ ) with different lengths depending on the required T-matching length ( $L_t$ ) and width ( $W_t$ ) [11], and the antenna is modeled with RLC series while the RFID IC is modeled by RC series.

The approximate values of components ( $R_{ant}$ ,  $L_{ant}$ ,  $L_{shunt}$ , and  $L_{series}$ ) were calculated using electric wall concept and Equations (1) and (2) [12].

$$L_{(a,m)} = \frac{\mu_0 l}{2\pi} \ln \left( \frac{l}{w} \right) + \frac{\pi}{2} \quad (1)$$

$$R_a = 80\pi^2 \alpha^2 \left( \frac{l}{\lambda} \right)^2 \quad (2)$$

The capacitance is calculated using the resonance frequency equation:

$$f = \frac{1}{2\pi \sqrt{L_a * C_a}} \quad (3)$$

The factor ( $\alpha$ ) in Equation (2) is calculated using Equation (4):

$$\alpha = \frac{1 - \cos \frac{\pi l}{\lambda}}{\frac{\pi L}{\lambda} \sin \frac{\pi l}{\lambda}} \quad (4)$$

The calculated values are an approximation; therefore, some components were tuned using ADS software.

### 3. BENDING EFFECT

The primary application of textile UHF RFID tags is in textile-concealed worn systems, which implies frequent bending and stretching [13]. Because of that, the read ranges of the RFID tag with different bending angles have been studied by using various cylindrical shapes with radius ranging from 35 mm to 50 mm. Three main radii were studied:  $R = 30$  mm,  $R = 35$  mm, and  $R = 50$  mm. Two different cases have been taken into account for each radius: concave and convex bending, see Figure 5.

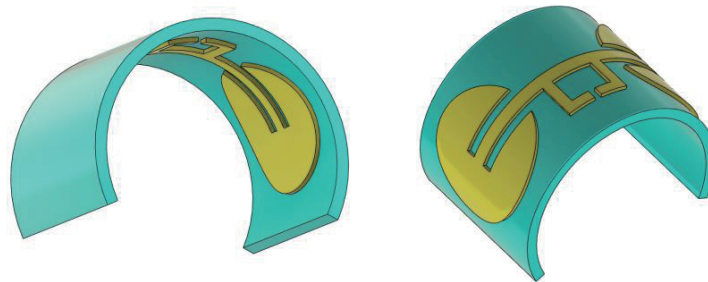


**Figure 5.** 3D view of the proposed design under concave and convex bending.

To estimate the effect of bending on the RFID tags, the read range ( $r$ ) was calculated using the Friis formula (5) and also by using the simulated gain ( $G_t$ ) of the tag antenna which is approximately equal to 2.196 dBi.

$$r = \frac{\lambda}{4\pi} \sqrt{\frac{P_t G_t G_r \tau}{P_{th}}} \tag{5}$$

Thing Magic M6e RFID reader performance was used to measure the read range. The reader antenna gain is  $G_r = 6$  dBi, and the chip sensitivity which is the minimum power required to activate the RFID IC is  $P_{th} = -8$  dBm, with  $\lambda$  being the free space wavelength and  $\tau$  the power transmission coefficient that is related to power reflection coefficient.

Figure 6 and Figure 7 show the predicted read range for concave and convex bending, respectively. The bending radius effect can be summarized as the higher the bending radius, the lower the effect on

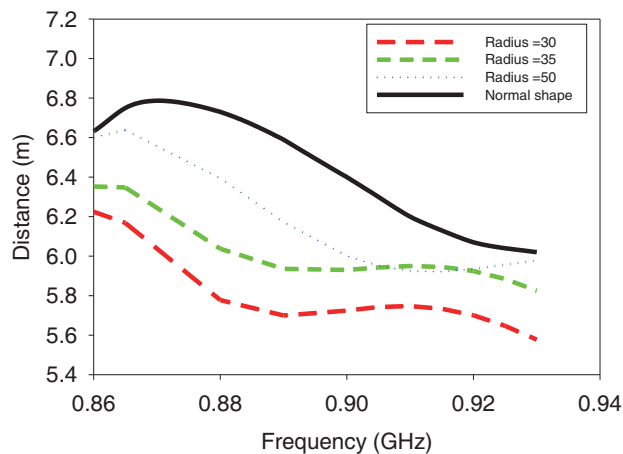


**Figure 6.** Read range convex.

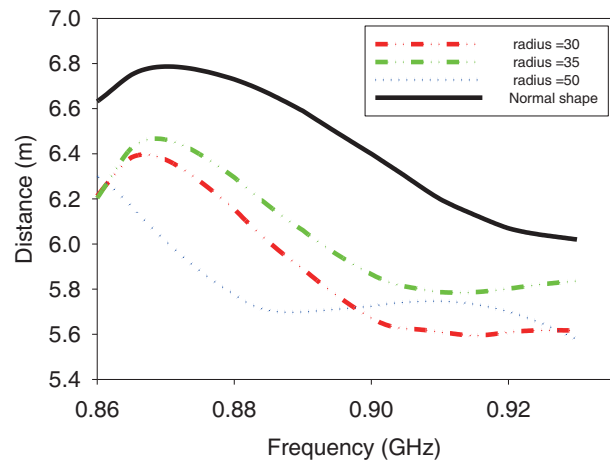


**Figure 7.** Read range concave.

the RFID tag read range. At 915 MHz, the read range achieved is 6.2 m without bending, and it drops to 5.6 m and 5.75 m for the maximum concave and convex bendings, respectively (radius 30 mm). It can be concluded that the convex bending has lower impact on the overall UHF RFID system performances.

#### 4. HUMAN BODY EFFECT

Biological tissues dissipate energy, and unlike the non-absorbent materials that can turn into EM energy reflectors, human body absorbs the electromagnetic radiation received from the RFID reader. Therefore, the energy received by the tag drops to a level that reduces the antenna gain by approximately 80%. As can be observed by analyzing the Friis formula (Equation (5)) the gain is a highly influencing parameter on the read range. Thus, any variation of the antenna gain can cause an increase or decrease of the read range, as shown in Figure 8. The simulated gain is reduced to a value between  $-4$  and  $-7$  dBi, hence the read range is also affected.

As shown in Figure 9, the high permittivity value that the Human body organs exhibit shifts the resonance frequency of the tag from 10 to 55 MHz and decreases the magnitude of the reflection coefficient by a value of more than 50% in comparison of the one in free space. Consequently, it causes a drop of the energy received by the RFID chip and minimizes the power sent back to the reader antenna.

The proposed design is intended to be used for the traceability of the elderly people as a wearable

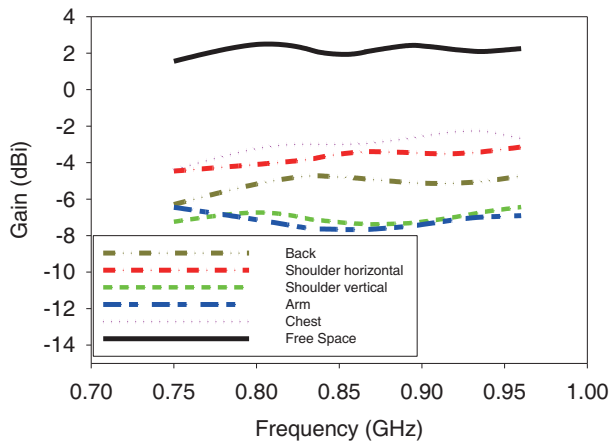


**Figure 8.** Gain over frequency for the tag in free space and on human body.

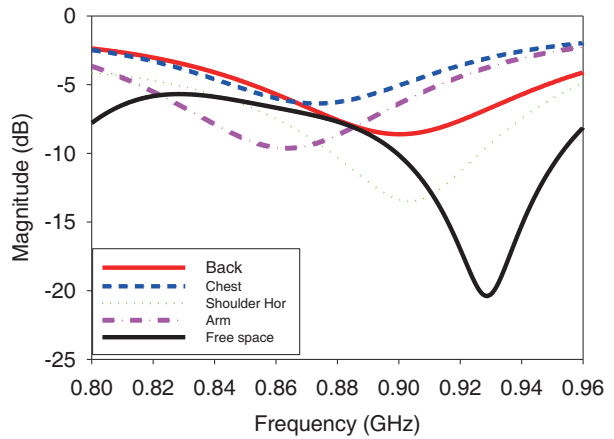


**Figure 9.** Simulated reflection coefficient on human body and for free space.

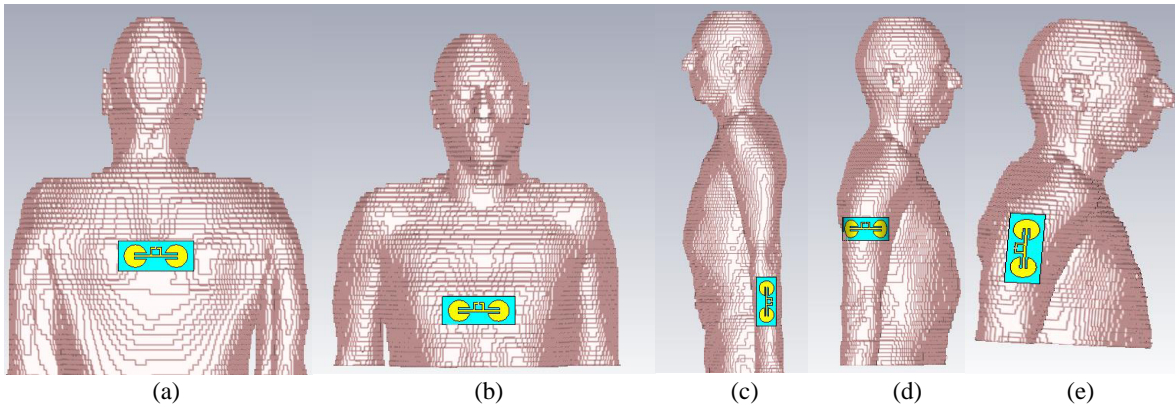


**Figure 10.** Simulation set-up of RFID tag on different positions of human body: (a) Back. (b) Chest. (c) Arm. (d) Shoulder vertical position. (e) Shoulder horizontal position.

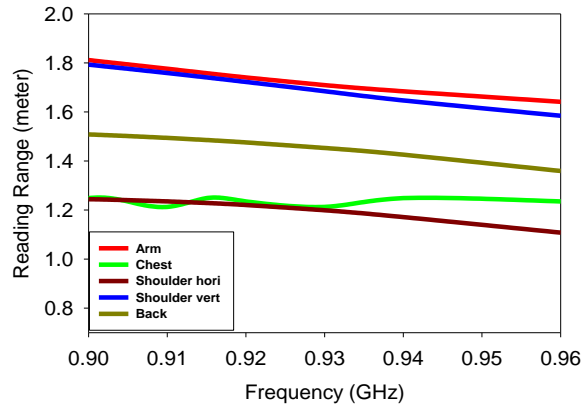


Figure 11. Simulated reading range of the RFID tag on different human body positions.

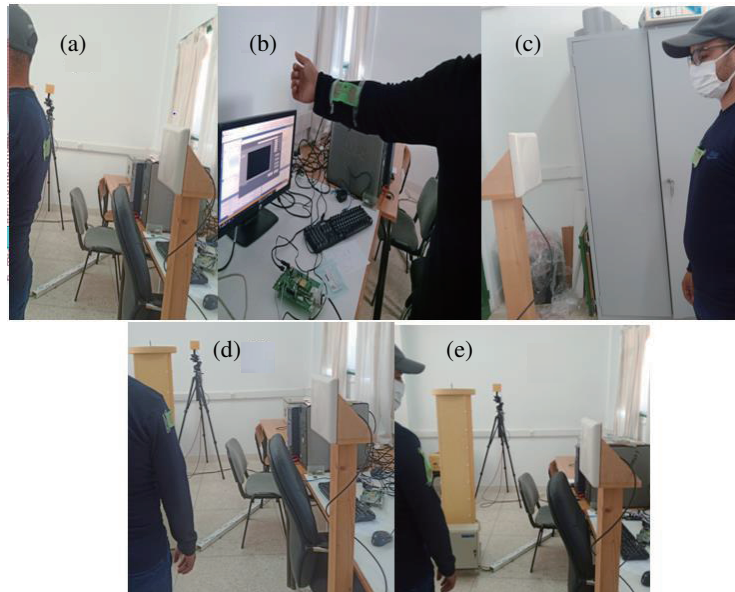


Figure 12. Experimental set-up for the tag measurements on different human body parts: (a) Back. (b) Arm. (c) Chest. (d) Shoulder vertical position. (e) Shoulder horizontal position.

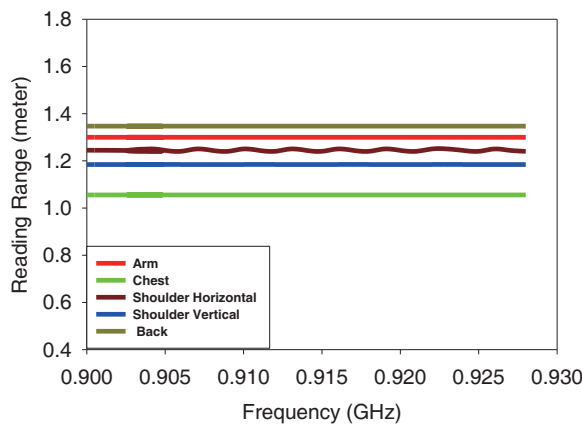


Figure 13. Measured reading range of the tag on different human body positions.

**Table 2.** Specific absorption rate (SAR) for the tag on different body location.

| Body parts          | SAR 1g (W/Kg) | SAR 10g (W/Kg) |
|---------------------|---------------|----------------|
| Chest               | 1.834         | 1.028          |
| Shoulder horizontal | 0.664         | 0.300          |
| shoulder vertical   | 24.570        | 6.644          |
| Back                | 27.194        | 3.651          |
| Arm                 | 17.791        | 17.791         |

technology. Nowadays, this technology has been used in many aspects of our daily life, such as electronic skins, body monitoring sensors, and other. The widespread use of this wearable devices poses new challenges such as their effect on the body. Thus, the SAR (specific absorption rate) value is simulated for the Gustav Voxel model (CST STUDIO 2020) [14] on different human body parts as shown in Figure 10. In order to locate the setups that comply with the regulation for general public exposure, it can be seen that for 1 g the safest disposition is for a tag aligned vertically on the shoulder where the SAR corresponds to 44% of the permitted SAR value, while for 10 g both the chest and vertical shoulder disposition do not exceed the limit and correspond to 51% and 15%, respectively (Table 2). Furthermore, we have simulated and measured the reading range on different human body parts as shown in Figure 10 and Figure 12. The obtained results are plotted in Figure 11 and Figure 13, respectively. We can clearly see that the reading range is sensitive to the position of the RFID tag on the human body.

## 5. CONCLUSION

We studied the effect of the bending and the human body proximity on the embroidered RFID tag. The tag is designed after identifying the effect of the parameters specific to the antenna structure. Also, the electric circuit modeling the antenna is elaborated in order to optimize the dimensions of the T-matching elements and achieve the required matching with the chip. The read range was measured for a tag located on different parts of an adult human body. The results showed that the read range was reduced by approximately 80% due to the human body dissipative characteristics. Finally, in order to verify the compliance of the system with the international standards, SAR values simulations were carried out for different wearable tag scenarios. the results showed that only particular locations kept the SAR level in the permitted limits. Future work includes study of the feasibility of embroidered tags with integrated sensing capabilities and the realization of embroidered ground planes on the tag structure in order to reduce the dissipative effect of the human body and the SAR.

## REFERENCES

1. Liukkonen, M., "RFID technology in manufacturing and supply chain," *International Journal of Computer Integrated Manufacturing*, Vol. 28, No. 8, 861–880, 2015.
2. Adame, T., A. Bel, A. Carreras, J. Melià-Seguí, M. Oliver, and R. Pous, "CUIDATS: An RFID-WSN hybrid monitoring system for smart health care environments," *Future Generation Computer Systems*, Vol. 78, Part 2, 602–615, 2018.
3. Mehmood, A., et al., "Body movement-based controlling through passive RFID integrated into clothing," *IEEE J. Radio Freq. Identif.*, Vol. 4, No. 4, 414–419, 2020.
4. Yu, M., X. Shang, M. Wang, Y. Liu, and T. T. Ye, "Exploiting embroidered UHF RFID antennas as deformation sensors," *IEEE J. Radio Freq. Identif.*, Vol. 4, No. 4, 406–413, 2020.
5. Ivsic, B., D. Bonafacic, and J. Bartolic, "Textile antennas for on-body sensors," *SAS 2015 — 2015 IEEE Sensors Appl. Symp. Proc.*, June 2015.
6. Koski, K., et al., "Practical read range evaluation of wearable embroidered UHF RFID tag," *IEEE Antennas Propag. Soc. AP-S Int. Symp.*, 2012.



7. Kellomäki, T., “On-body performance of a wearable single-layer RFID tag,” *IEEE Antennas Wirel. Propag. Lett.*, Vol. 11, 73–76, 2012.
8. Oyeka, D. O., J. C. Batchelor, and A. M. Ziai, “Effect of skin dielectric properties on the read range of epidermal ultra-high frequency radio-frequency identification tags,” *Healthc. Technol. Lett.*, Vol. 4, No. 2, 78–81, 2017.
9. Rahman, N. H. A., Y. Yamada, and M. S. A. Nordin, “Analysis on the effects of the human body on the performance of electro-textile antennas for wearable monitoring and tracking application,” *Materials (Basel)*, Vol. 12, No. 10, 1–17, 2019.
10. Marrocco, G., “The art of UHF RFID antenna design: Impedance-matching and size-reduction techniques,” *IEEE Antennas Propag. Mag.*, Vol. 50, No. 1, 66–79, 2008.
11. Sockolov, K. and D. Arakaki, “UHF RFID antenna impedance matching techniques,” *2017 IEEE Antennas Propag. Soc. Int. Symp. Proc.*, 2433–2434, 2017.
12. Sohrab, A. P., Y. Huang, M. Hussein, M. Kod, and P. Carter, “A UHF RFID tag with improved performance on liquid bottles,” *IEEE Antennas Wirel. Propag. Lett.*, Vol. 15, 1673–1676, 2016.
13. El Bakkali, M., M. Martinez-Estrada, R. Fernandez-Garcia, I. Gil, and O. El Mrabet, “Effect of bending on a textile UHF-RFID tag antenna,” *14th Eur. Conf. Antennas Propagation, EuCAP 2020*, 2020.
14. CST STUDIO SUITE CST AG, Germany, [www.cst.com](http://www.cst.com).